

# Uplift Load Monitoring for Two Bored Piles in Shrink-swell Soil

Jean-Louis Briaud, Professor, Texas A&M University, College Station, TX, USA; email: <a href="mailto:briaud@tamu.edu">briaud@tamu.edu</a> Jerome Sfeir, Ph.D. Student, Texas A&M University, College Station, TX, USA; email: <a href="mailto:jeromesfeir@tamu.edu">jeromesfeir@tamu.edu</a>

**ABSTRACT:** The swelling and shrinking of high plasticity clays can induce significant loads in otherwise stress-free piles such as bored piles right after construction. The seasonal weather fluctuations through rainfall and sunshine induce changes in water content and thus vertical movements, which lead to uplift by swelling or downdrag due to shrinking in the bored piles over time. This article describes three case histories in three different locations where measurements of load distributions in bored piles constructed in high plasticity clays were conducted along with associated undrained shear strength laboratory tests. The maximum friction generated due to swelling and due to shrinking is back-calculated from the measured loads, and recommendations are proposed to estimate the maximum friction using the undrained shear strength of the clay.

**KEYWORDS:** Uplift, Bored pile, Drilled shaft, Shrink-swell soils, Full scale test, Load test, Tension, Fine grain soils, Expansive clays.

SITE LOCATION: Geographic Database

### INTRODUCTION

When a bored pile or drilled shaft is constructed in a fine grain soil which goes through seasonal swelling and shrinking, it can be loaded in tension as the upper part of the pile is pulled up during the swelling of the fine grain soil and the bottom part of the pile resists that uplift. This condition may happen, for example, when the soil is a shrink-swell fine grain soil, the ground water table is 5 m deep, and the bored pile is 15 m long. In this case, the swelling zone is likely associated with the upper 5 m, and the resisting zone is the bottom 10 m of the pile. The tension load in the pile impacts the amount of reinforcement necessary and this condition must be evaluated at the design stage. The question addressed in this article is how much friction can be generated by the swelling and shrinking of the upper fine grain soil layer.

### BASIC PHENOMENON

Figure 1 shows an example of the axial load profile as the uplift is generated in the case of no load at the top of the pile. In this case, the dead weight of the pile is neglected. In the upper swelling zone, the active zone, the tension load increases from zero (at the surface) down to the bottom of the active zone (where it reaches a maximum value). Then the load decreases to zero in the non-swelling zone which resists the uplift. From the movement point of view, two elements are considered: the pile and the soil. The pile is loaded upward, and thus an upward pile movement develops at the ground surface. Because of the rigidity of the pile, the movement profile of the pile is close to linear and decreasing with depth. The soil is moving upward in the active zone due to the swelling process likely to occur in the wet season. In that active zone, the upward movement of the soil is larger than the upward movement of the pile and generates an uplift friction on the pile. Below the active zone, the soil movement is also upward as it resists the upward movement of the pile. However, the upward soil movement is smaller than the upward pile movement as the soil generates downward friction on the pile.

Submitted: 25 September 2023; Published: 30 October 2025

Reference: Briaud J.-L., and Sfeir J. (2025). *Uplift Load Monitoring for Two Bored Piles in Shrink-swell Soil*. International Journal of Geoengineering Case Histories, Volume 8, Issue 3, p. 55-70, doi: 10.4417/IJGCH-08-03-04



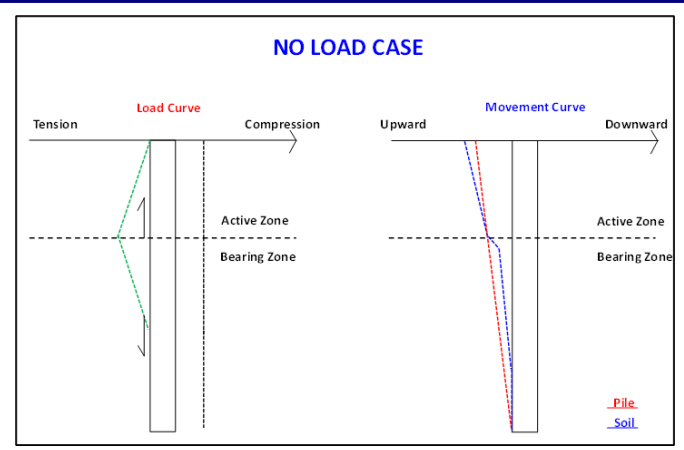


Fig. 1 – Load in drilled shaft – no load case.

Figure 2 shows an example of the axial load profile in the case of a large compression load at the top of the pile after the uplift is generated. The large compression load dominates the response of the pile, and the pile is in compression all the way to the bottom of the pile. In the active zone, the soil movement is upward due to swelling—but, because the pile goes down, the friction on the pile is upward. Below the active zone, the soil movement is downward but less than the pile movement, as it is reacting to the downward movement of the pile; the friction is upward as well.

In many cases, such as buildings and bridges, the large compression load applied at the end of construction is likely to create the condition shown in Figure 2. However, there are cases such as with oil tanks where the tank may be nearly empty several times during its service life; in this case, the condition of Figure 1 is created. For such cases, it is important to be able to estimate the maximum uplift friction that the fine grain soil can generate on the pile. A few recommendations exist.

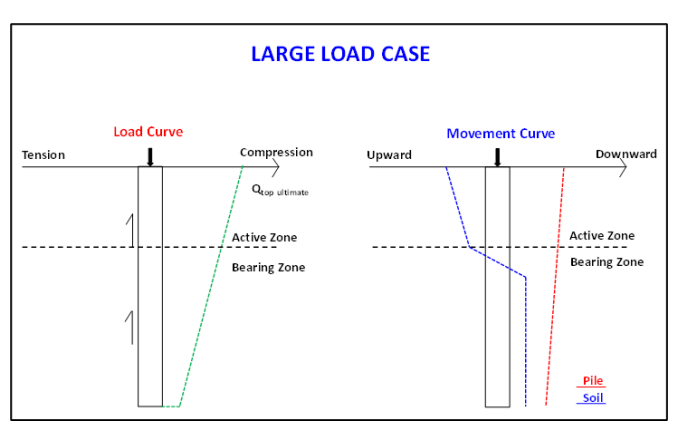


Fig. 2 – Load in drilled shaft – large compression load case.

### **EXISTING KNOWLEDGE**

When a pile is loaded downward, the maximum friction resistance  $f_{max}$  of a fine grain soil is usually related to the undrained shear strength  $s_u$  through an  $\alpha$  factor. This is a total stress approach to the problem.

$$f_{\text{max}} = \alpha s_{\text{u}}$$
 (1)

For bored piles and stiffer fine grain soil, the  $\alpha$  value is often taken as 0.5 (Brown et al, 2010). One question is to know if this  $\alpha$  value also applies to the case where the fine grain soil swells and applies an upward friction on the pile. In the swelling case, Brown et al. (2010) suggest that  $\alpha$  should be equal to 1, and that the  $s_u$  value should be evaluated at the water content of the soil or rock after it absorbs all the water possible under the overburden pressure corresponding to the depth



below finished grade. We will refer to this  $s_u$  value as the fully softened undrained shear strength of the fine grain soil. The Foundation Performance Association (2017) suggests that the  $\alpha$  value should be the same as the one used for the resistance in non-swelling fine grain soils as shown below:

$$\alpha = 0.55 \qquad \qquad \text{for} \qquad \qquad s_u < 150 \text{ kPa} \tag{2}$$

$$\alpha = 0.55 - 0.1((s_u/100) - 1.5)$$
 for  $150 \text{ kPa} < s_u < 250 \text{ kPa}$  (3)

Johnson and Stroman (1982) suggest that  $\alpha$  should be 0.5 for stiff non-swelling fine grain soils but could approach 1 for swelling fine grain soils as the soil expands tightly against the pile. In an effort to use an effective stress approach to the problem, O'Neill (1988) proposed to estimate  $f_{max}$  as:

$$f_{\text{max}} = \beta_1 \, \sigma'_s \tan \varphi_r \tag{4}$$

where  $\beta_1$  is a factor larger than 1 to account for soil disturbance and soil-structure interaction,  $\sigma'_s$  is the swelling pressure in terms of effective stress, and  $\phi_r$  is the residual strength effective stress friction angle. Around the same time Chen (1988) proposed a similar expression:

$$f_{\text{max}} = \beta_2 \, \sigma'_{\text{s}} \tag{5}$$

where  $\beta_2$  is a coefficient of uplift between the pile and the soil. Thus  $\beta_2 = \beta_1 \tan \phi_r$ . Chen (1988) states that  $\beta_2 = 0.15$  is a reasonable value, based on laboratory experiments. O'Neill suggests a value of 1.3 for  $\beta_1$ . So, if  $\phi_r$  varies between 5° and 10°, then  $\beta_1$  tan  $\phi_r$  varies between 0.11 and 0.23. The value of  $\sigma'_s$  is typically measured in a consolidometer test with inundation while preventing swell. While the water stress is not typically measured in that test, it may be reasonable to assume that it ends up being zero at the end of the test. In this case, the total stress swell pressure is equal to the effective stress swell pressure  $\sigma'_s$ .

The other issue is to estimate the depth of the active zone  $z_a$  within which the fine grain soil will swell. There have been several recommendations regarding estimating  $z_a$ , none of which are decisively practical. Among some of the recommendations for  $z_a$  are the depth of the cracks in the fine grain soil, the depth to where the soil changes color, the depth to the ground water level, the depth to where the water tension (suction) becomes constant over time, and the depth to where the water content becomes constant over time. All these have their value but are not always practical for a given project. Estimating  $z_a$  was the topic of a recent effort in which numerical simulations were undertaken (Chen et al., 2019). While the numerical simulations indicated the stronger influence of some soil parameters like the hydraulic conductivity, they did not result in simple recommendations. At the end of this project, a map was prepared based on a survey of common practices of 13 major geotechnical firms in Texas (Figure 3).



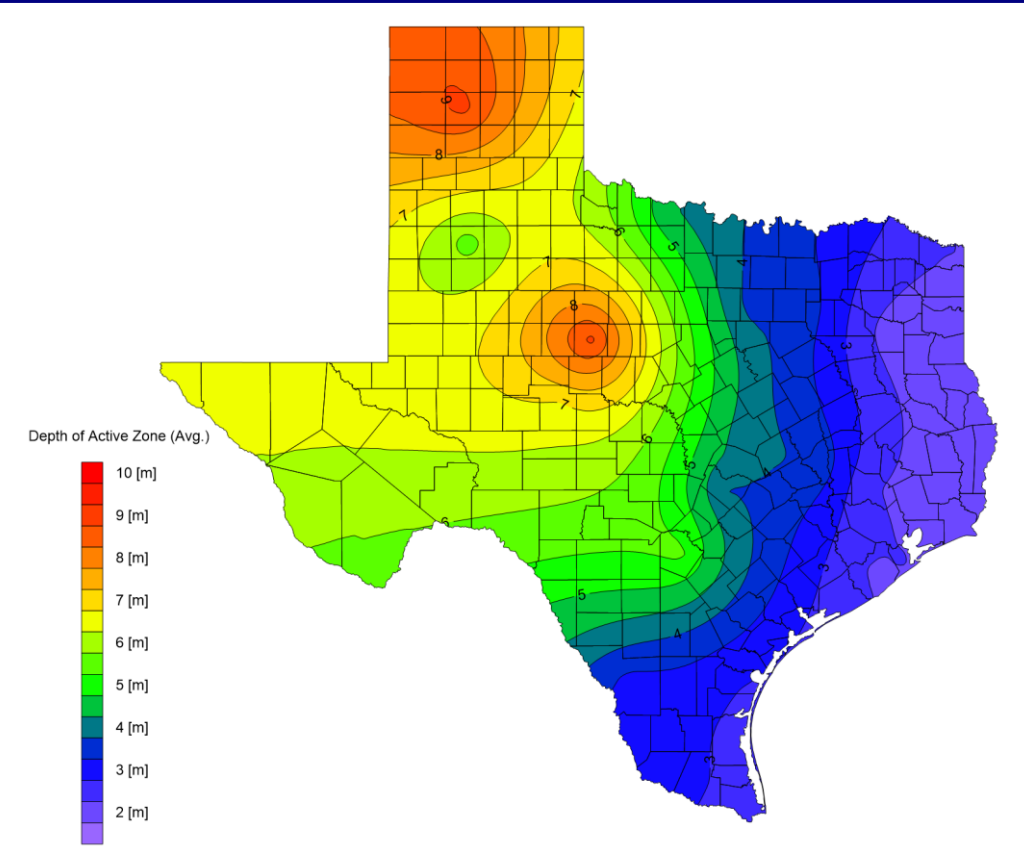


Fig. 3 – Map of active depth in Texas based on practitioner survey (Chen et al., 2019).

### TWO EXISTING CASE HISTORIES

Two full-scale case histories were identified where bored piles were drilled in a shrink-swell fine grain soil and subjected to inundation and seasonal variations for a relatively long period of time and where the load was measured or inferred. They are Johnson and Stroman (1982) and Da Silva Burke et al. (2022).

### Johnson and Stroman (1982) Case History

In July 1966, 7 reinforced concrete bored piles were constructed at the Lackland Air Force Base in Texas as part of a bored piles in fine grain soil research project by the USACE. Bored pile No. 2 (LAFB-2) is of particular interest for the topic of this article (see Figure 4). LAFB-2 is 0.762 m in diameter with a 1.22 m diameter 60° bell at the bottom. The total length of the pile below ground is 10.98 m, including the 0.61 m high bell.

The soil surrounding the pile was inundated in 1966 for 11 months after construction. The soil at the site is made of a 2.29 m thick layer of clay (CH), below which is a 1.52 m thick layer of clayey gravel (GC), underlain by a clayey shale (CH) extending well past the bottom of the pile. A ground water level is found at a depth of 2.44 m, a level which can fluctuate over time by as much as 1.22 m. The top clay layer has the following average properties (Figure 5): water content = 28%, dry unit weight = 14.62 kN/m³, plasticity index = 43%, undrained shear strength = 60 kPa, effective stress friction angle = 25°, swell pressure = 86 kPa, pressuremeter limit pressure = 330 kPa, and cone penetrometer point resistance = 1290 kPa. The clayey gravel has the following average properties: water content = 28%, undrained shear strength = 86 kPa, and cone penetrometer point resistance = 5530 kPa. The clay shale layer has the following average properties: water content = 30%, dry unit weight = 14.78 kN/m³, plasticity index = 55%, undrained shear strength = 182 kPa, effective stress friction angle = 29°, swell pressure = 287 kPa, pressuremeter limit pressure > 1500 kPa, and cone penetrometer point resistance = 4900 kPa.

The soil movement and the pile movement were monitored with respect to a 21 m deep benchmark. In 1974, not quite a year after the soil around the pile was inundated, the soil surface had heaved 107 mm and the pile head 63 mm. By 1981,



the soil surface had heaved 196 mm and the pile head 86 mm. A compression load test was conducted on pile LAFB-2 in 1982. The load settlement curve is shown in Figure 4. As can be seen, the curve exhibits an intermediate plunging failure around 2224 kN with additional resistance developing after 50 mm settlement on to a final plunging load of 3470 kN. Johnson (1984) interprets this dual plunging failure as overcoming the friction on the pile at a load of 2224 kN with an additional 1246 kN associated with the resistance of the 1.22 m diameter bell shape base.

Johnson (1984) further interprets, based on differential heave measurements between the bottom of the pile and the soil movement at the level of the bottom of the pile, that a gap had developed between the bottom of the bell and the soil below. As such, one can use 2224 kN as the ultimate uplift friction load on the pile and back-calculate the maximum uplift friction stress  $f_{max}$  as 84.6 kPa (2224 /  $\pi$  x 0.762 x 10.98). This assumes that friction develops along the bell as well as the pile shaft. This value is to be compared with the weighted average undrained shear strength along the shaft of the pile, or 143.2 kPa ((60x2.29+86x1.52+182x7.17)/10.98). The back-calculated  $\alpha$  value for this case history is 0.59 (84.6/143.2). For the effective stress approach, if an effective stress swell pressure of 150 kPa is selected from Figure 5, the back-calculated  $\beta_2$  value in Eq.5 is 0.56, much higher than the 0.15 value suggested.

# a) PILE LAFB-2 AND STRATIGRAPHY

0.45

10.3

# Clay Overburden (CH) 2.3 Clayey Gravel (GC) Clayey Shale (CH)

# b) LOAD TEST CURVE

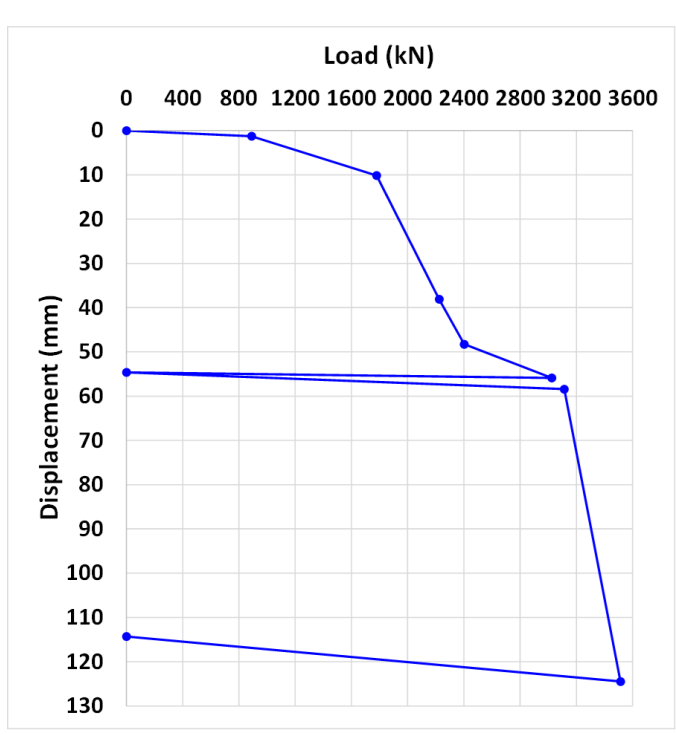


Fig. 4 – Johnson and Stroman (1982) case history: (a) dimensions of pile LAFB-2 and stratigraphy, (b) load test result (Johnson, 1984).



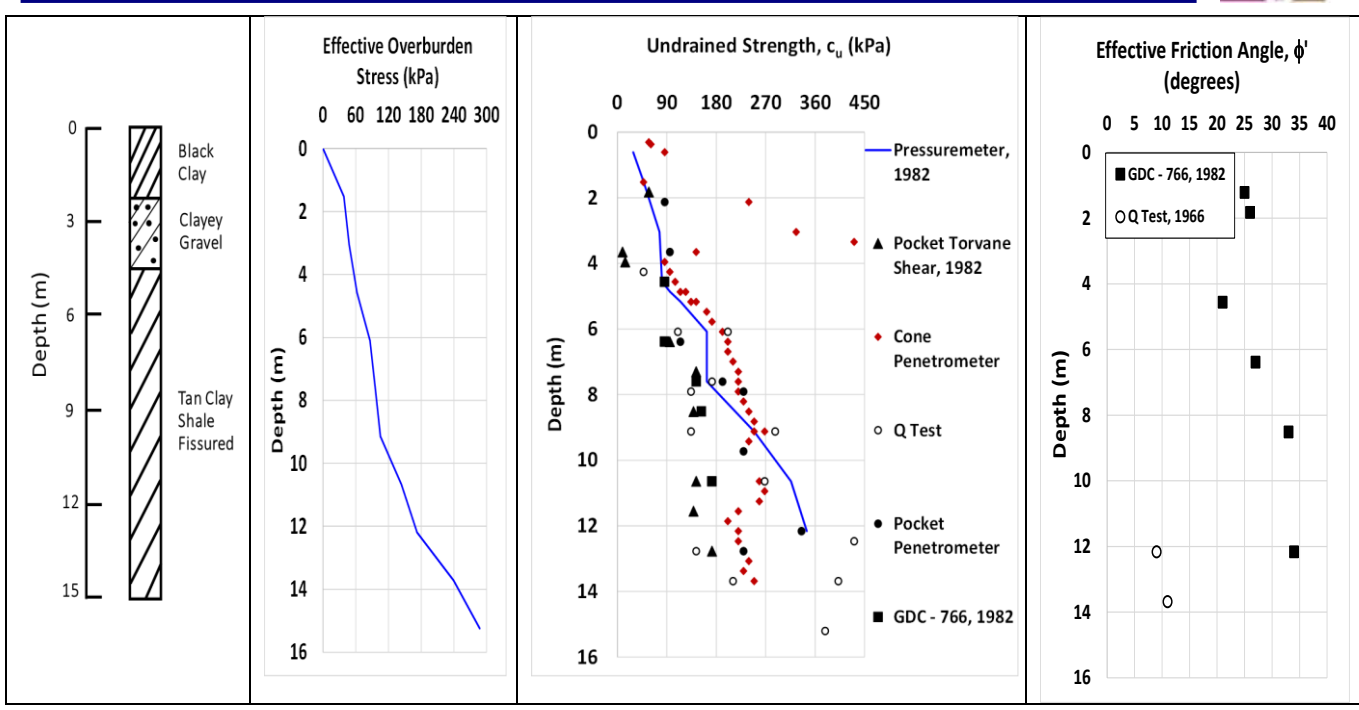


Fig. 5a – Soil properties near pile LAFB No.2 (Johnson, 1984). GDC-766 is a boring number.

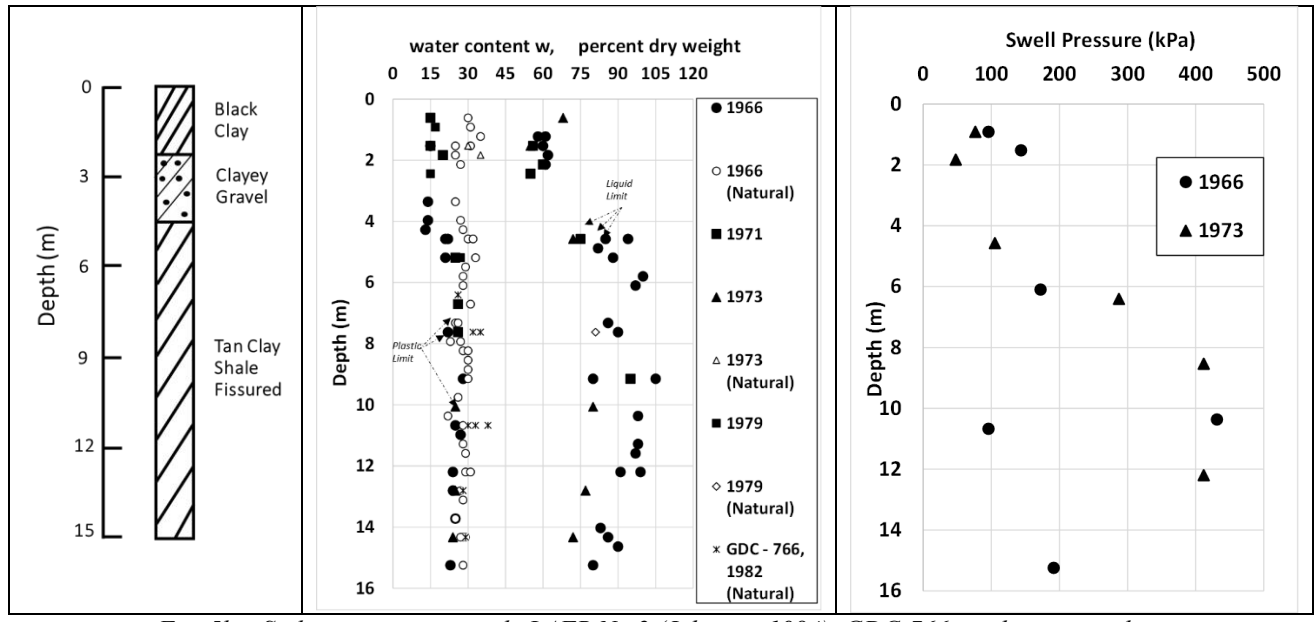


Fig. 5b – Soil properties near pile LAFB No.2 (Johnson, 1984). GDC-766 is a boring number.

### Da Silva Burke et al. (2022) Case History

In January 2020, two identical bored piles were constructed in South Africa between the towns of Kroonstad and Vredefort. The piles were 50 m apart, with one being the reference pile and the other one being the test pile. They were 450 mm in diameter and 16.5 m long below the ground surface, including a 1 m socket in the base rock (Figure 6). The piles were instrumented with 6 levels of vibrating wire strain gages to obtain the load in the pile as a function of depth. The test pile was inundated for 6 months and monitored for 11 months. No free water was found in the sampling boreholes. Water tension (suction) was measured to be 1 MPa and 0.43 MPa at 1.95 and 6.45 m depth respectively and 0 MPa below that.



The soil at the site is made of a 4 m thick layer of swelling clay. Below this is a 3 m thick layer of another swelling clay with a higher sand content. Further below lies a 8.5 m thick layer of sand, underlain by a very soft rock (Figure 6). The average properties of the swelling clay (top 7 m) are: initial water content = 21.5%, dry unit weight = 14.2 kN/m³, initial degree of saturation = 68.3%, liquid limit = 79%, plasticity index = 40.5%, effective stress friction angle = 26°, effective stress cohesion = 5 kPa, cone penetrometer (CPT) point resistance = 3860 kPa, and undrained shear strength inferred from CPT = 206 kPa (Da Silva Burke et al., 2022, using Robertson, 2010). Figure 7 shows the CPT results.

The heave of the ground surface was 59 mm around the inundated pile at the end of the test period of 11 months. The ground surface around the non-inundated pile settled with a maximum shrinkage of 3.9 mm. As a result, the inundated pile was subjected to tension in the upper soil zone (Figure 8) while the non-inundated pile was subjected to compression in the upper soil zone (Figure 9). In Figures 8 and 9, tension loads are positive, and compression loads negative.

Figures 8 and 9 also show the soil-pile interface friction (upward soil friction positive) calculated from the load distribution profiles along the two piles. The maximum friction  $f_{max}$  reached values as high as 70 kPa in uplift along the inundated pile, while it reached values as high as 120 kPa in downdrag along the non-inundated pile. This indicates that shrinkage loading was more severe in this case than swelling loading. However, compression is not as impactful as tension for bored reinforced concrete piles. Considering the CPT based estimate of the undrained shear strength of 206 kPa, the back-calculated  $\alpha$  value is 0.34 for the inundated test pile (uplift by swelling) and 0.58 for the not-inundated reference pile (downdrag by shrinkage), which is 1.71 times higher than the swelling value. It was also observed during this case history that the inundated test pile was subjected not only to uplift load but also to significant bending, attributed to uneven swelling of the clay.

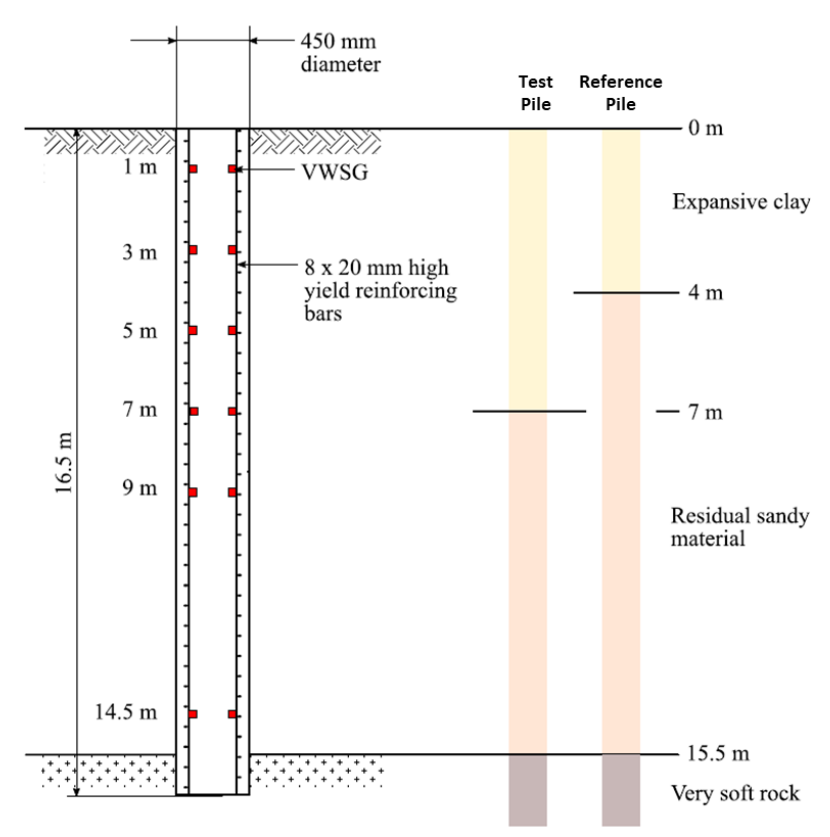


Fig. 6 – Dimensions of the pile and stratigraphy (Da Silva et al., 2022).

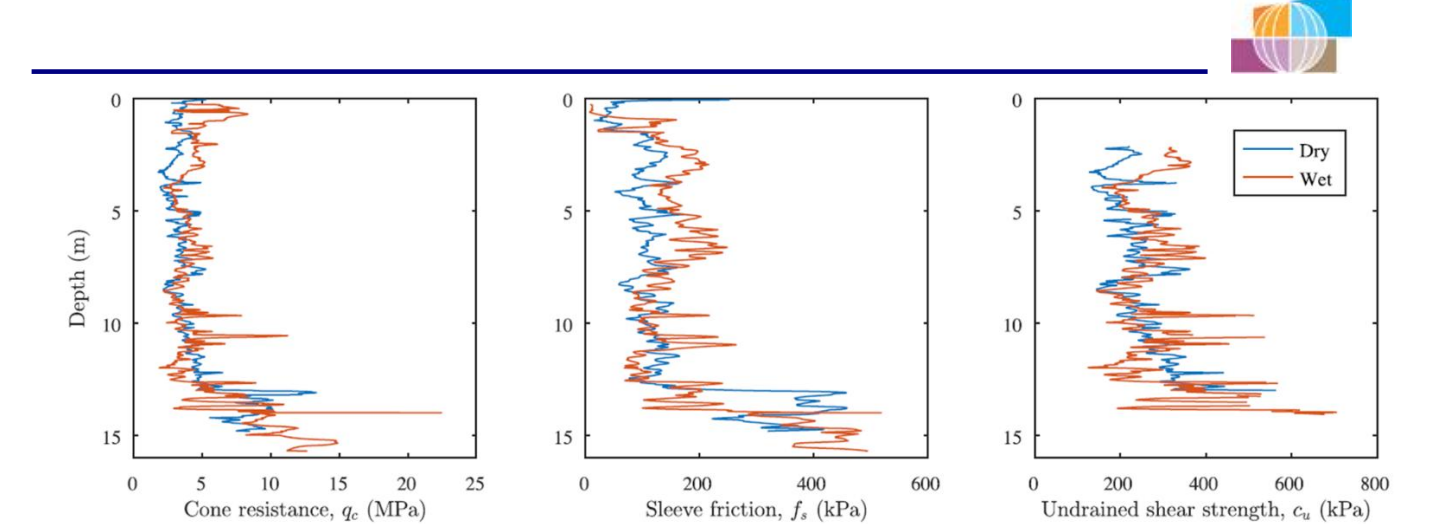


Fig. 7 - CPT results and inferred undrained shear strength (Da Silva Burke et al., 2022).

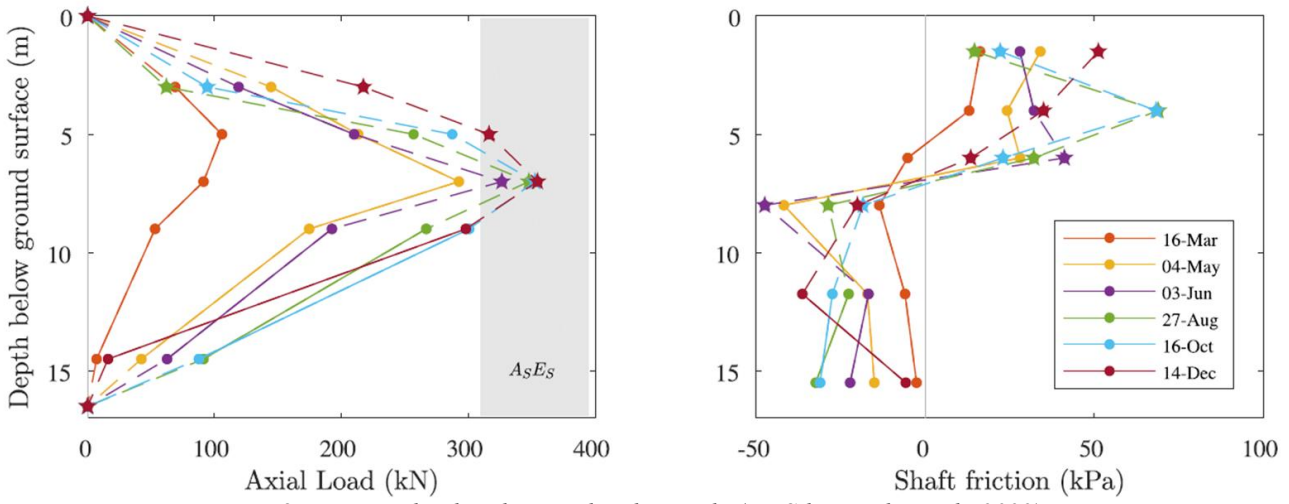


Fig. 8 – Tension load in the inundated test pile (Da Silva Burke et al., 2022).

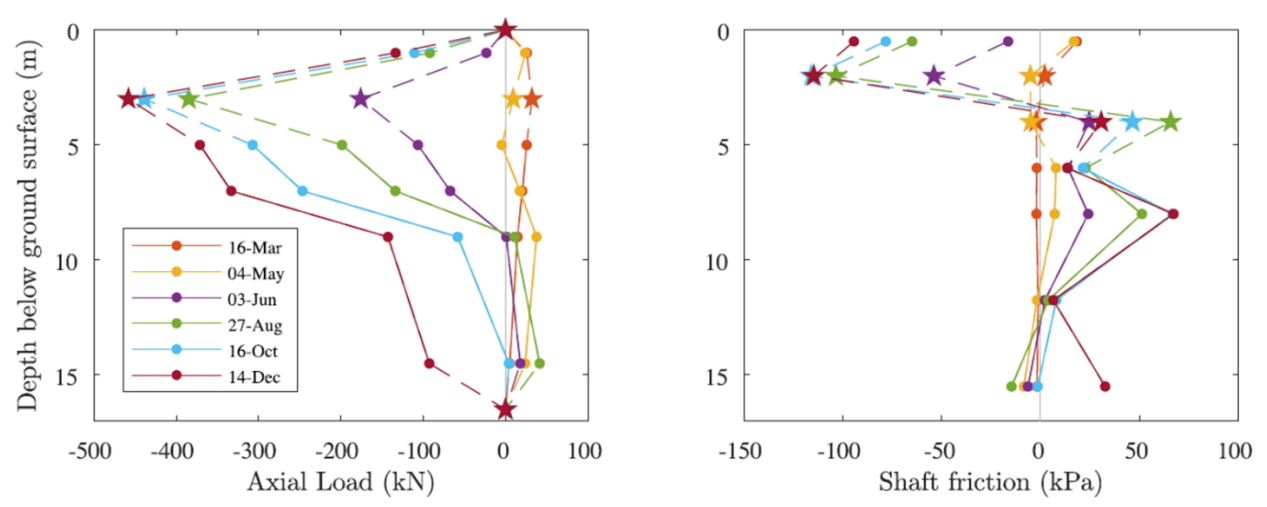


Fig. 9 – Compression load in the non-inundated reference pile (Da Silva Burke et al., 2022).

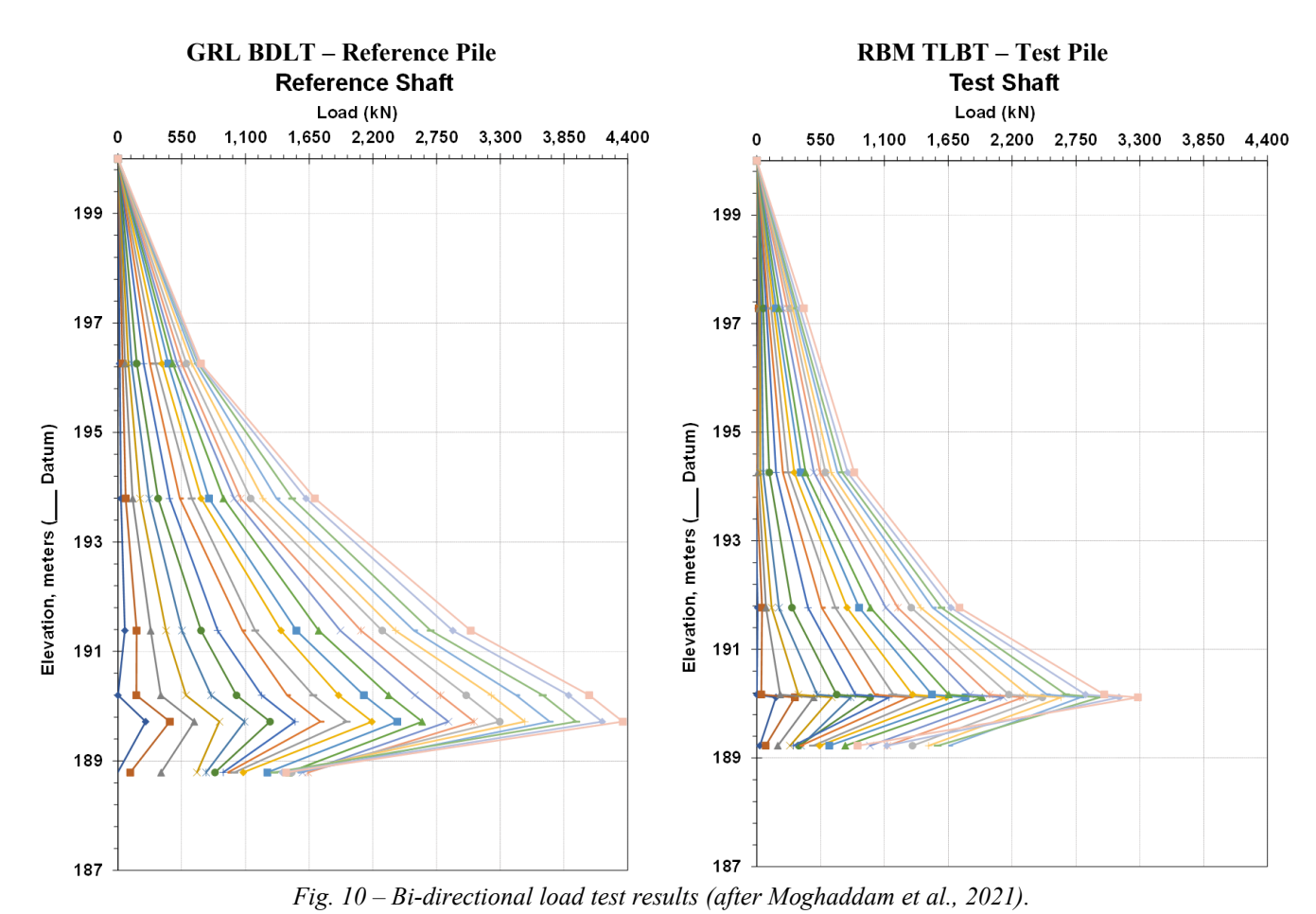


# SAN ANTONIO CASE HISTORY

### The Piles

After reviewing the existing literature and analyzing the two case histories of Johnson (1984) and Da Silva et al. (2022), it was decided in 2022 to undertake the full-scale monitoring of two bored piles constructed in 2020 at the A.H. Beck yard in Converse, Texas, near San Antonio. The two piles are 1.22 m in diameter, 10.67 m long below the ground surface, and spaced 4.57 m center to center. One pile would serve as a reference pile and the other would be the test pile with the soil around it being inundated. In 2020, bi-directional load tests were conducted on the piles using two different systems: (1) the conventional Bi-Directional Load Test, or BLDT (Osterberg load cell type); and (2) a new Top Loaded Bidirectional Test, or TLBT.

The BDLT was performed by the GRL company on the reference pile by placing the load cell hydraulic jack at a depth of 9.15 m below ground within the pile, and the TLBT was performed by the RBM company on the test pile by placing two plates at a depth of 9.15 m within the pile and applying the bi-directional load from the top of the pile. The results of the load tests are shown in Figure 10. Only the top 9.15 m part of the two piles was monitored during this shrink-swell study. As such, the top three levels of vibrating wire strain gages are of interest in this study; they are respectively located at 3.75 m, 6.22 m, and 8.63 m depth below ground surface for the reference pile, and at 2.71 m, 5.73 m, and 8.23 m for the test pile.





### The Soil

The soil at the site is a high plasticity clay (CH) with the following average properties: water content = 25%, dry unit weight =  $15.9 \text{ kN/m}^3$ , liquid limit = 65%, and plasticity index = 44%. The ground water level in 2020 was found at a depth of 6.7 m. Direct shear tests were performed on clay samples at Texas A&M University; unconsolidated undrained triaxial tests were also performed at Intertek-PSI. Rapid loading was imposed to obtain the undrained shear strength of the clay. Figure 11 shows these results, along with the undrained shear strength values obtained from the pocket penetrometer test ( $s_u = 0.35x(PPT \text{ reading})$ ) and from tests where, in the direct shear test, the sample was inundated and left to swell freely vertically for 24 hours before shearing.

The average of the not-inundated undrained shear strengths measured with the direct shear test and the triaxial test within the top 5 m of the clay deposit is 79.4 kPa. The ratio of the average of the 24 hour inundated samples undrained shear strength over the average of the not-inundated samples undrained shear strength was 0.57. Free swell tests were performed in the consolidometer, and the first set of samples showed practically no swell. The second set of samples showed changes in height equal to 0.6% and 3.5%. A free shrink test was then performed, and the relative change in volume was 25% after 7 days of air drying, and then 31% after 24 hours in the oven. Intertek-PSI performed some swell pressure tests indicating a best estimate of the swell pressure of 200 kPa.

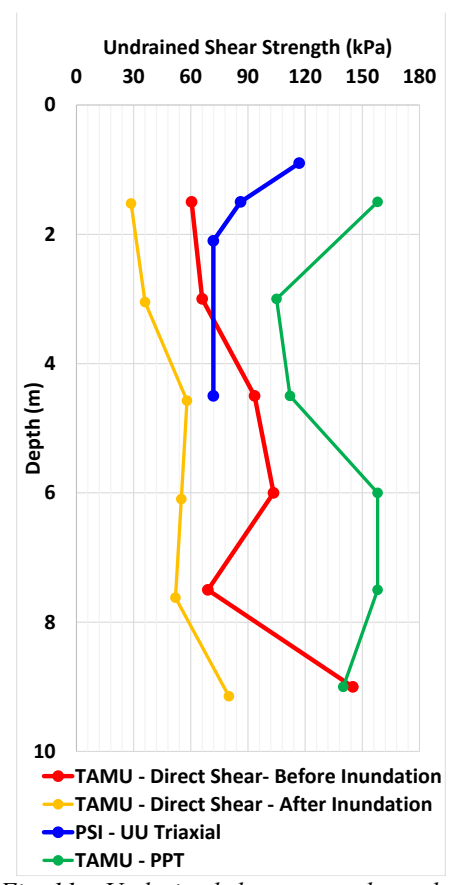


Fig. 11 – Undrained shear strength results.

# The Sequence of Events

The sequence of events at the site is shown in Figure 12. After the construction of the two bored piles and the bi-directional load tests in 2020, a 12.2 m deep benchmark was installed 5 m away from each pile in June 2022 (see Figure 13). The zero readings of the strain gages prior to the load tests were used for determining the loads in the piles observed as a function of time in 2022 and 2023. Readings of the strain gages in both piles and zero readings of the elevation targets were taken



using high precision (0.3 mm) surveying instruments in July 2022. Right after those readings were taken, a 3.66 m diameter and 1 m high casing was installed around the test pile and flooded with water to a height of 0.6 m above ground (Figure 13).

Readings of the three levels of strain gages in each pile and of the 10 elevation targets were read regularly for 11 months until June 2023. These elevation targets (see Figure 14) included the soil surface, the top of the piles, and the top of the casing. Very little vertical swelling movement, 1 mm maximum, was measured on any of the targets. This was thought to be due to the water in the large diameter casing not penetrating in the clay. In October 2022, four 4.57 m deep, 0.1 m diameter boreholes were drilled around the test pile within the 3.66 m diameter casing to facilitate water access at depth around the test pile.

In March 2023, after concerns of the possible drifting of the zero strain gage readings recorded prior to the bi-directional load tests, a trench was excavated around the reference pile down to 8.5 m to free the reference pile over the three levels of strain gages. New zero readings were recorded on the reference pile, indicating some definite shift in the zero readings between 2020 and 2022. This was surprising, as vibrating wire strain gages are usually quite stable. These new zero readings were used to obtain the loads in the reference pile. The same shift in zero readings was applied to the strain gages of the test pile. The final readings were taken on June 20, 2023.

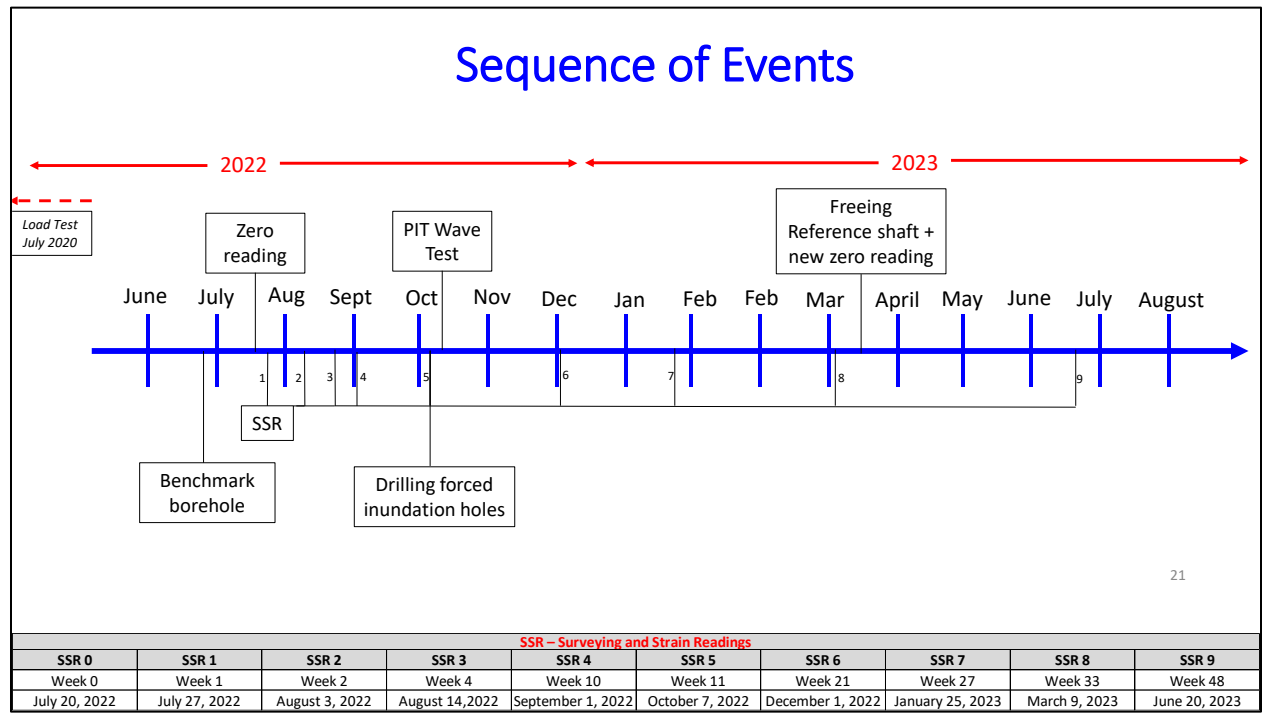


Fig. 12 – Sequence of events at the test site.





Fig. 13 – Test set up.

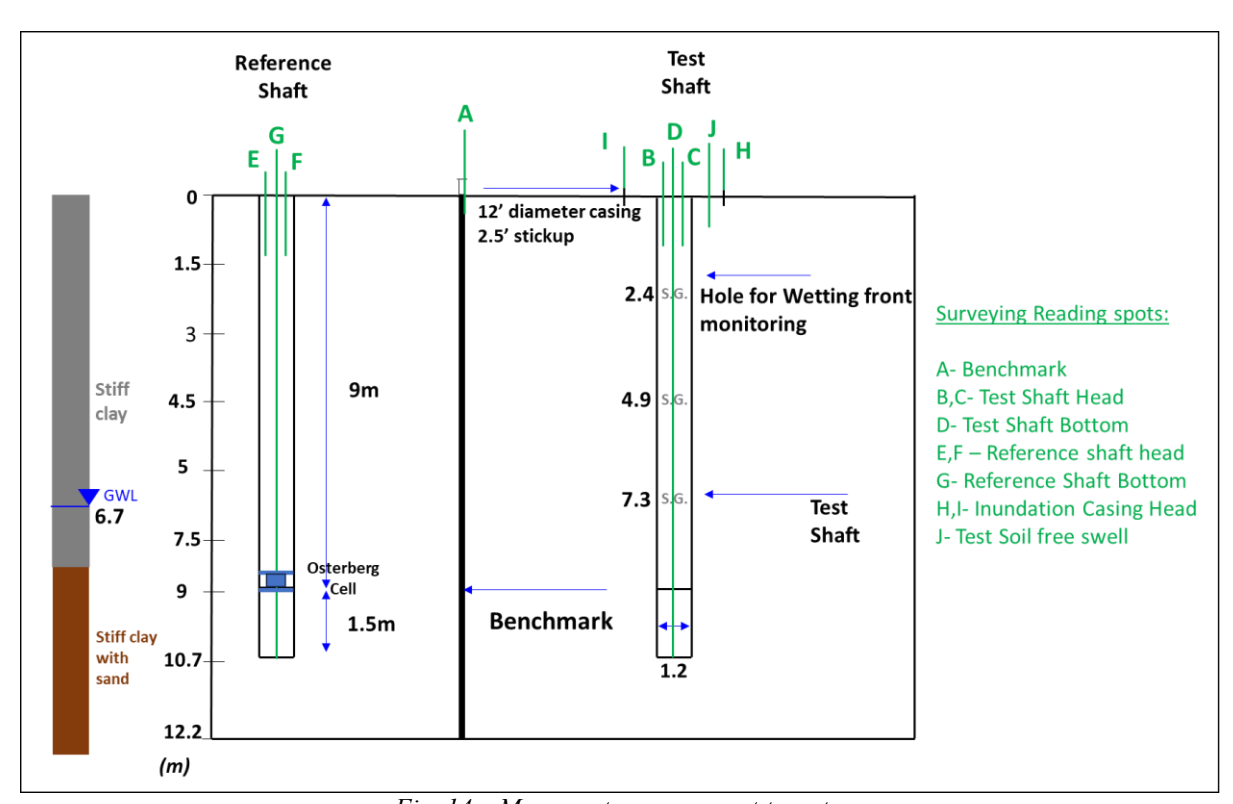


Fig. 14 – Movement measurement targets.

### **Test Results**

The strain gages attached to the reinforcement bars measure the strain  $\varepsilon$  in the pile at the location of the gage. To obtain the load Q from the gage readings, the pile rigidity AE is required.

$$Q = AE\varepsilon \tag{6}$$



where Q is the load in the pile at a depth z, A is the cross section area of the pile, E is the modulus of the pile material, and  $\varepsilon$  is the normal strain in the pile at that depth. For reinforced piles, a composite rigidity made of concrete and steel is considered, and:

$$AE = A_{s}E_{s} + A_{c}E_{c} \tag{7}$$

where  $A_s$  and  $A_c$  are the cross sections of steel and concrete respectively, and  $E_s$  and  $E_c$  are the modulus of steel and concrete respectively.

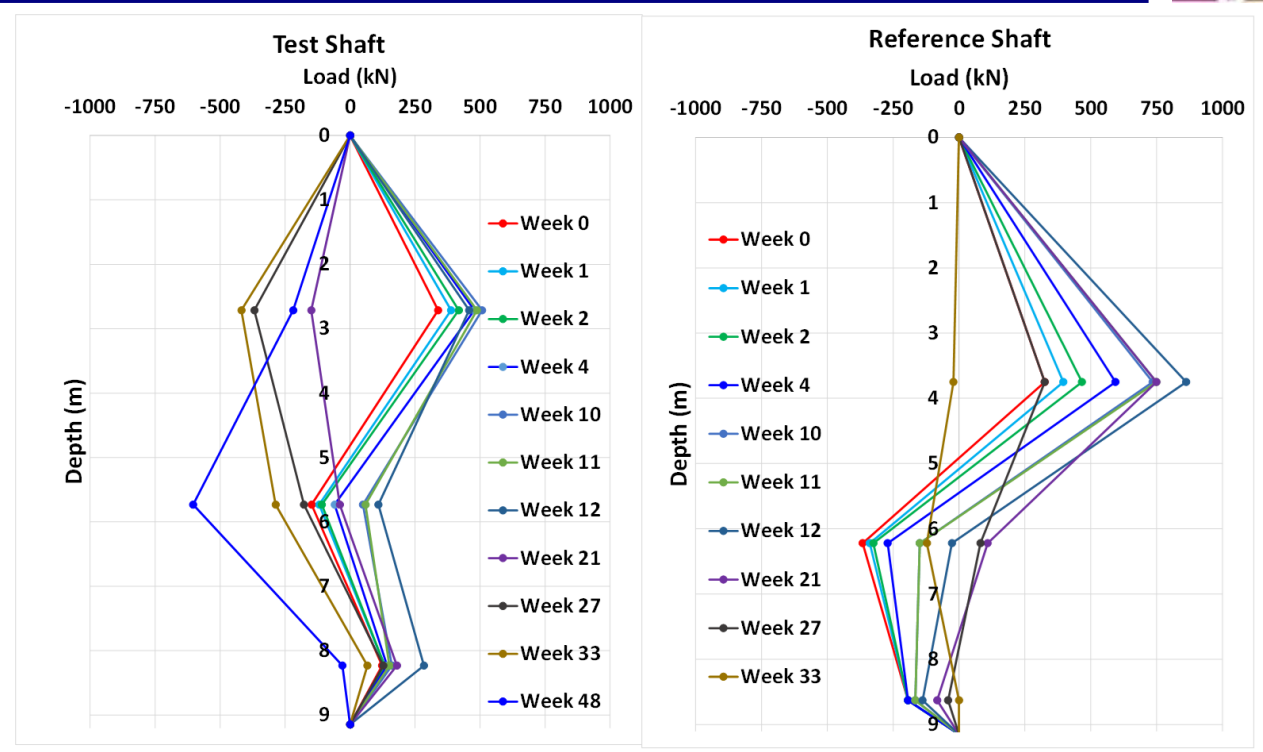
One question remained about the modulus of concrete in tension: Is it the same as in compression? Neville (1965) ran parallel tension and compression tests on concrete cylinders, and found that the two moduli were the same if the tensile strain was less than 100 microstrains. Since this was the case for this project, the same modulus was used in compression and in tension. In the end, the AE values for the test pile were 27761 MN for the first level of strain gages, 27712 MN for the second level of strain gages, and 26551 MN for the third level of strain gages. The AE values for the reference pile were 39660 MN for the first level of strain gages, 37708 MN for the second level of strain gages, and 38922 MN for the third level of strain gages. The load distributions in the reference pile and the test pile are shown in Figure 15, along with their evolution over the time of observation from July 2022 to June 2023.

Figure 16 shows the same data, plus the load test results at maximum load as well as the residual loads after bringing back the load to zero following the load test. In Figures 15 and 16, compression loads are positive, and tension loads are negative. Figure 17 shows the evolution of the load at the depth of the first strain gage versus time in both piles. As can be seen, the piles were in compression when the monitoring started in July 2022. This is attributed to shrinkage of the soil over the top 5 m of the piles during Spring 2022 and the start of Summer 2022. The interface friction between the soil and the pile was back-calculated from the load distributions in Figure 15 and is shown in Figure 18 for the maximum friction values measured.

The maximum friction in shrinkage downdrag was recorded for the reference pile and reached 83.6 kPa. Since the average undrained shear strength within that zone was 79.4 kPa, this gives an  $\alpha$  value for shrinkage downdrag of 1.05. The maximum friction in swelling uplift was recorded for the test pile and gave 40.3 kPa; this gives an  $\alpha$  value for swelling uplift of 0.51. However, if the undrained shear strength obtained after inundating the sample for 24 hours prior to shearing is used, the  $\alpha$  value becomes 0.89. So, the maximum friction in shrinkage downdrag was almost twice as large as the maximum friction in swelling uplift.

Note that from week 33 to week 48, or for almost 4 months, the wet front had propagated much lower and induced uplift down to the second strain gage, or a depth of 5.73 m. Note also that the compression load in the top part of the reference pile reduced from about 1200 kN down to 311 kN, which may indicate that the reference pile was being impacted by the water inundating the test pile. The water level in the soil around the test pile moved up from a depth of 6.7 m in 2017, to 5.3 m in mid-2022, to 1.83 m at the end of the observation period.





*Fig.* 15 – Load distribution in both piles.

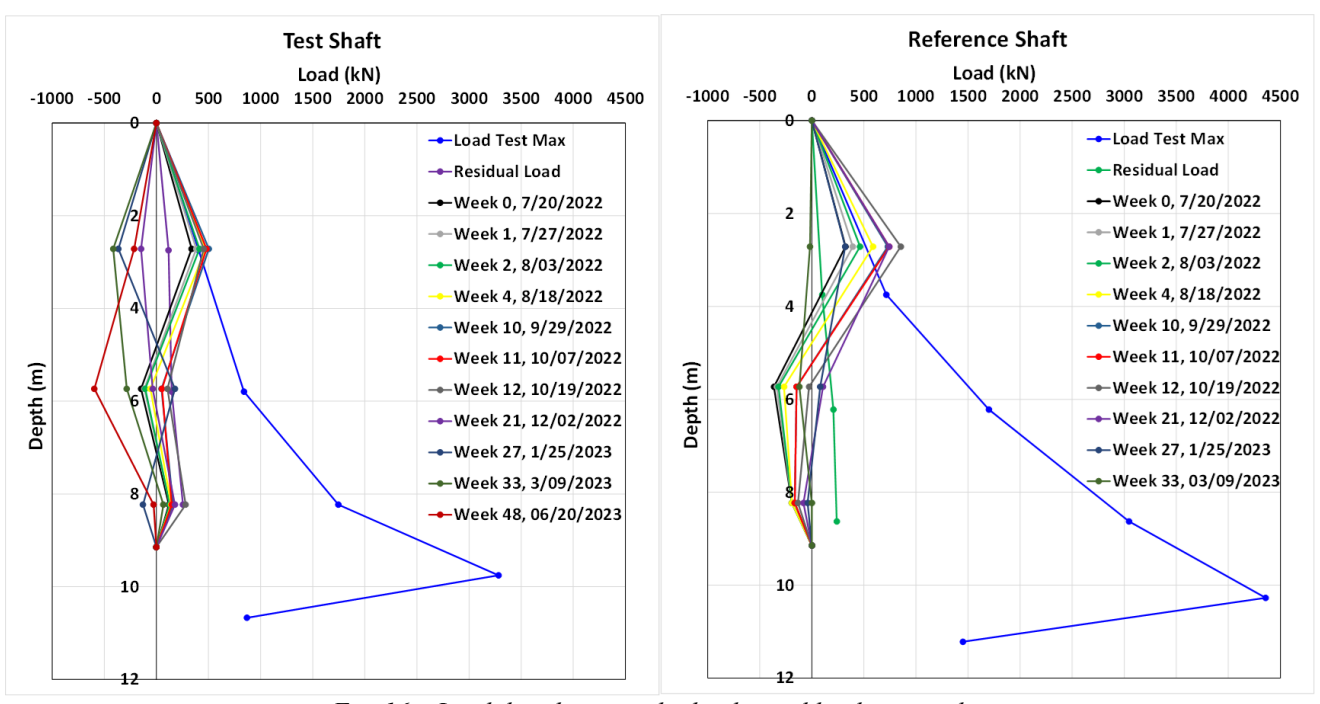


Fig. 16 – Load distribution in both piles and load test results.



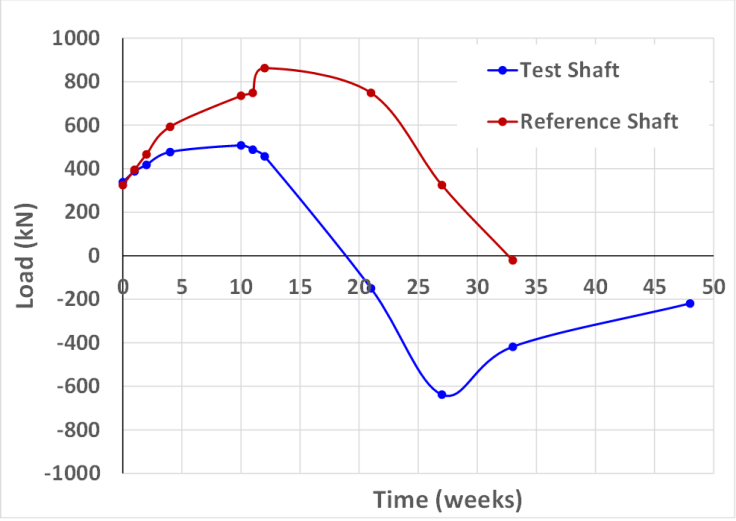


Fig. 17 – Evolution of the load in the piles at the depth of the first strain gage (2.71 m deep for the test pile and 3.75 m depth for the reference pile).

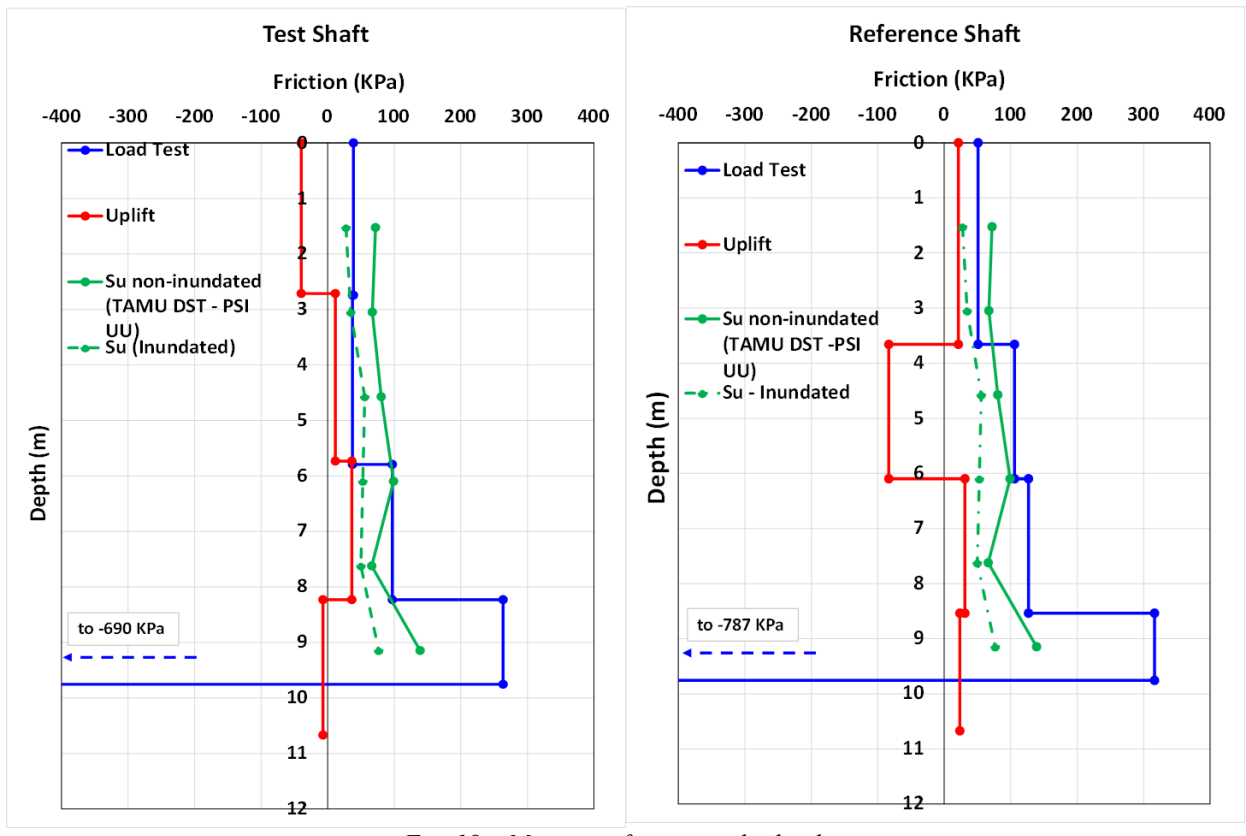


Fig. 18 – Maximum friction on both piles.

# **CONCLUSIONS**

Three case histories are presented, dealing with the uplift friction generated by swelling clays on bored piles. Two are reported in the literature: the Lackland Air Force Base case and the South Africa case. One is presented in this article: the San Antonio case. The goal of the project was to recommend  $\alpha$  values for maximum uplift friction as in  $f_{max} = \alpha s_u$ . The



Lackland Air Force Base case gave an  $\alpha$  value of 0.59, the South Africa case gave an  $\alpha$  value of 0.34, and the San Antonio case gave an  $\alpha$  value of 0.51 for an average  $\alpha$  value very close to 0.5.

Also, the South Africa case and the San Antonio case gave  $\alpha$  values for the maximum downdrag friction generated by shrinking clays which were 1.71 and 2.06 times larger than the maximum uplift friction generated by swelling clays respectively. It is suspected that this is impacted by the fact that the undrained shear strength of the soil increases when the water content decreases, and not necessarily in a change of  $\alpha$  value. The San Antonio case showed that the undrained shear strength of the clay after 24 hours' inundation before shearing was 0.57 times the undrained shear strength without inundation. This gave an  $\alpha$  value of 0.89. Thus, based on the limited measurements presented in this article, it seems reasonable to recommend the following alpha values:

- $\alpha = 0.5$  for swelling uplift friction when using the not-inundated undrained shear strength.
- $\alpha = 1.0$  for swelling uplift friction when using the undrained shear strength where the sample is inundated for 24 hours before shearing.
- $\alpha = 1.0$  for shrinking downdrag friction when using the not-inundated undrained shear strength.

### **ACKNOWLEDGEMENTS**

This project was sponsored by CERGEP, the Consortium for Education and Research in Geo-Engineering Practice at Texas A&M University. The members are A.H. Beck, Corsair, ECS, Fugro, Geosyntec, Intertek-PSI, Kiewit, Menard, Odin, Paradigm, Reinforced Earth, Raba Kistner, Riner Engr., and Terracon. We wish to thank, in particular, Tracy Brettmann at A.H. Beck and Shailendra Endley at Intertek-PSI for their significant help during the field work of this project.

### REFERENCES

- Brown D., Turner J., Castelli R. (2010). "Drilled Shafts: Construction Procedures and LFRD Design Methods", NHI Course No. 132014, *Geotechnical Engineering Circular No. 10*, Washington, D.C., USA.
- Chen Y., Sanchez M., Briaud J.-L. (2019). "Predicting ground surface movement for shrink-swell soil", CERGEP Report No.8 SI units, Consortium for Education and Research in Geo-Engineering Practice, Department of Civil Engineering, Texas A&M University, College Station, Texas, USA, 73 pages.
- Da Silva Burke, T.S., Jacobsz, S.W., Elshafie, M.Z.E.B, Osman, A.S. (2022). "Measurement of pile uplift forces due to soil heave in expansive clays." *Canadian Geotechnical Journal*.
- Foundation Performance Association. (2017). "Design Procedure for Drilled Concrete Piers in Expansive Soils", Report by the Structural Committee, Houston, Texas, Document # FPA-SC-16-0, www.foundationperformance.org
- Johnson L.D. (1984). "Methodology for design and construction of drilled shaft in cohesive soils", Technical Report GL-84-5, US Army Engineer Waterways Experiment Station, US Army Corps of Engineers, Vicksburg, Miss., USA.
- Johnson L.-D., Stroman W. (1982). "Long-Term Behavior of a Drilled Shaft in Expansive Soil", *Transportation Research Record*, 1032.
- Moghaddam, R. B., Hannigan, P. J., Rausche, F. (2021). "Top-Loaded Bi-Directional Test and the Conventional Bi-Directional Load Test, A Direct Comparison." *Proc.*, 46th Annual Conference of the Deep Foundation Institute, DFI, Chicago, Illinois, USA.
- Robertson P.K. (2010). "Soil behavior type from CPT: an update", *Proc., 2nd Int. Symp. on Cone Penetration Testing* (CPT'10), CPT'10 Organizing Committee, 575-583.



The Journal's Open Access Mission is generously supported by the following Organizations:









Access the content of the ISSMGE International Journal of Geoengineering Case Histories at: <a href="https://www.geocasehistoriesjournal.org">https://www.geocasehistoriesjournal.org</a>

Downloaded: Tuesday, December 02 2025, 18:16:16 UTC